MOLECULAR AND CELLULAR BIOLOGY, Dec. 2010, p. 5787–5794 Vol. 30, No. 24
0270-7306/10/$12.00 doi:10.1128/MCB.00347-10
Copyright © 2010, American Society for Microbiology. All Rights Reserved.

Requirement of the ATM/p53 Tumor Suppressor Pathway for Glucose Homeostasis[▽]

Heather L. Armata,[1,2] Diane Golebiowski,[1] Dae Young Jung,[2,3] Hwi Jin Ko,[2,3] Jason K. Kim,[2,3,4] and Hayla K. Sluss[1,2]*

Department of Medicine,[1] Division of Endocrinology, Metabolism and Diabetes,[2] and Program in Molecular Medicine,[4] University of Massachusetts Medical School, Worcester, Massachusetts 01605, and Department of Cellular and Molecular Physiology, Pennsylvania State University College of Medicine, Hershey, Pennsylvania 17033[3]

Received 24 March 2010/Returned for modification 26 April 2010/Accepted 7 October 2010

Ataxia telangiectasia (A-T) patients can develop multiple clinical pathologies, including neuronal degeneration, an elevated risk of cancer, telangiectasias, and growth retardation. Patients with A-T can also exhibit an increased risk of insulin resistance and type 2 diabetes. The ATM protein kinase, the product of the gene mutated in A-T patients (*Atm*), has been implicated in metabolic disease, which is characterized by insulin resistance and increased cholesterol and lipid levels, blood pressure, and atherosclerosis. ATM phosphorylates the p53 tumor suppressor on a site (Ser15) that regulates transcription activity. To test whether the ATM pathway that regulates insulin resistance is mediated by p53 phosphorylation, we examined insulin sensitivity in mice with a germ line mutation that replaces the p53 phosphorylation site with alanine. The loss of p53 Ser18 (murine Ser15) led to increased metabolic stress, including severe defects in glucose homeostasis. The mice developed glucose intolerance and insulin resistance. The insulin resistance correlated with the loss of antioxidant gene expression and decreased insulin signaling. *N*-Acetyl cysteine (NAC) treatment restored insulin signaling in late-passage primary fibroblasts. The addition of an antioxidant in the diet rendered the p53 Ser18-deficient mice glucose tolerant. This analysis demonstrates that p53 phosphorylation on an ATM site is an important mechanism in the physiological regulation of glucose homeostasis.

Ataxia telangiectasia (A-T) is a recessive progeroid disease of early childhood, with poor prognosis. Patients can develop a constellation of clinical pathologies, including neuronal degeneration, an elevated risk of cancer, telangiectasias, accelerated aging, growth retardation, and pulmonary disease (25). In addition, A-T patients exhibit an increased risk of insulin resistance and type 2 diabetes (3). The gene mutated in A-T patients (*Atm*) encodes a protein kinase that phosphorylates the p53 tumor suppressor on a site (Ser15) that regulates transcription activity (10, 21, 43). The loss of *Atm* has been implicated in metabolic disease, which is characterized by insulin resistance and increased cholesterol and lipid levels, blood pressure, and atherosclerosis (42).

Studies have attributed most of the pathology in A-T patients and *Atm*-deficient cells to increased levels of reactive oxygen species (ROS) and oxidative stress (4, 15, 20). Thus, the loss of ATM function has been hypothesized to lead to a state of chronic oxidative stress, which can contribute to insulin resistance. However, how ATM senses ROS levels is not clear. p53 has been shown to have a dual role in the regulation of reactive oxygen species, a major source of cellular stress (8, 27, 35). On one hand, very high levels of p53 (such as in overexpression studies) or high levels of stress will induce p53-dependent prooxidant genes (36), which can facilitate apoptosis. On the other hand, endogenous levels of p53 have been shown to regulate antioxidant gene expression (9, 38). Perhaps more physiologically relevant is the observation that p53 induces a transcriptional program in response to mild stresses, which may operate during physiological aging (46). Studies demonstrate a role of endogenous p53 levels in the regulation of genes involved in antioxidant defense, such as those encoding the sestrins (*Sesn*) (9) and glutathione peroxidase 1 (*GPX-1*) (38). Therefore, ATM and p53 both regulate the levels of ROS *in vivo*.

The development of insulin resistance in patients with A-T and in *Atm* mutant mice is poorly understood. ATM is activated by a number of stresses that have a direct impact on metabolism. A number of these cellular stresses, including atherosclerosis, trauma, hypoxia, and infections, are associated with p53 activation (12, 30, 32, 39, 44, 50, 51). Many of these stresses also cause phosphorylation of p53 on the ATM site (Ser15 in humans, Ser18 in mice). ATM-mediated p53 phosphorylation therefore represents a possible mechanism of physiological regulation of insulin sensitivity.

Additional support for p53 in regulating the metabolic effects of ATM has come from studies investigating the role of p53 in energy metabolism (7). p53 has been shown *in vitro* and *in vivo* to regulate the expression of genes involved in metabolism, such as the cytochrome *c* oxidase 2 gene (*Sco2*), which is required for mitochondrial respiration (29), glucose transporter genes, including *Glut1* and *Glut4*, in cancer cell lines (41, 48), the phosphoglycerate mutase gene (*PGM*) (24), *Tigar* (7), and the gene encoding which is zinc finger protein 385a (*Zfp385a*, also known as *hzf*), involved in adipocyte function and glucose homeostasis (22). p53 has been implicated in the

* Corresponding author. Mailing address: Department of Medicine, LRB 370W, University of Massachusetts Medical School, 364 Plantation St., Worcester, MA 01655. Phone: (508) 856-3372. Fax: (508) 856-3210. E-mail: hayla.sluss@umassmed.edu.

▽ Published ahead of print on 18 October 2010.

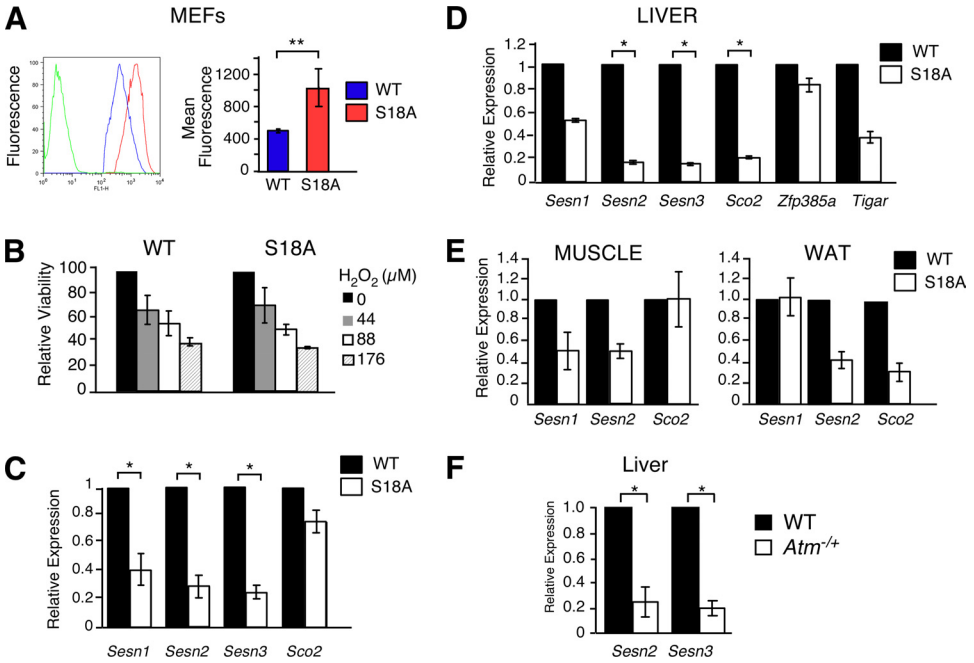

FIG. 1. Regulation of antioxidant and metabolic genes by p53 Ser18. (A) The amount of reactive oxygen species (ROS) in MEFs was examined by DCF staining and analysis by flow cytometry. Left, representative relative fluorescence of non-DCF-stained cells (green line) and DCF-stained wild-type (WT) (blue line) and p53 S18A (red line) cells; right, quantification of fluorescence. Data are presented as means ± standard errors of the means (SEM; $n = 5$). (B) Viability of MEFs treated with hydrogen peroxide at the indicated doses and harvested 18 h posttreatment. Data are presented as means ± SEM ($n = 5$). (C to F) The expression of *Sesn1*, *-2*, and *-3*, *Sco2*, or *Zfp385a*, and *Gapdh* mRNA was measured by quantitative real-time PCR analysis of the MEFs, liver, white adipose tissue (WAT), and skeletal muscle of 6- to 7-month-old wild-type mice and compared to that of $p53^{S18A}$ mice (C to E) and $Atm^{-/+}$ mice (F). The amount of *Gapdh* mRNA in each sample was used to calculate relative mRNA expression (means ± SEM; $n = 3$). Statistically significant differences between WT and $p53^{S18A}$ mice are indicated (*, $P < 0.05$).

development of insulin resistance through the regulation of senescence in adipose tissue (31). p53 has also been implicated in autoimmune disease and the macrophage response in a streptozotocin-induced type 1 diabetes model (52). Mice deficient for p53 were found to be more susceptible to streptozotocin-induced diabetes than wild-type mice. Thus, p53 had a protective role in this system. Although the p53 tumor suppressor has been implicated in the streptozotocin model of type 1 diabetes, the role of p53 in type 2 diabetes and insulin resistance has not been established.

The connection of p53 activity and p53 Ser18 phosphorylation to metabolic regulation supports a model whereby the mechanism of ATM-mediated physiological regulation of insulin sensitivity may involve p53 activity and ATM-mediated p53 phosphorylation. To test this hypothesis, we compared metabolic regulation in mice without and with a germ line mutation in the p53 phosphorylation site Ser18. These $p53^{S18A}$ mice exhibit defects in p53-mediated apoptosis and gene expression (10, 43), but unlike *p53*-null mice, $p53^{S18A}$ mice develop tumors only at advanced age (1). Analysis of various metabolic parameters indicated that $p53^{S18A}$ mice have increased metabolic stress. This metabolic deregulation is likely mediated through increased levels of ROS, as antioxidant treatment restores insulin sensitivity. Indeed, we observed impaired glucose homeostasis and insulin resistance in these animals, indicating that p53 Ser18 participates in a metabolic checkpoint.

MATERIALS AND METHODS

Mouse strains and diet information. The methods employed for the generation and genotyping of $p53^{S18A}$ mice (43), $p53^{-/-}$ mice (11), and $Atm^{+/-}$ mice (5) have been reported previously. $p53^{S18A/+}$ mice were intercrossed to obtain $p53^{S18A/S18A}$, $p53^{S18A/+}$, and $p53^{+/+}$ (wild-type) mice. Cohorts of male mice on a mixed 129/Sv × C57BL/6 genetic background were established for analysis. The mice were maintained on a standard chow diet. For antioxidant treatment, mice were given a diet containing 1.5% butylated hydroxyanisole (BHA; Bioserv; custom diet). All mice were housed in specific-pathogen-free facilities accredited by the American Association for Laboratory Animal Care. The Institutional Animal Care and Use Committees of the University of Massachusetts Medical School and Pennsylvania State University approved all studies using animals.

Glucose and insulin tolerance tests. Mice were examined using a glucose tolerance test (GTT) and an insulin tolerance test (ITT) with methods described previously (33). Mice were fasted overnight and challenged by the intraperitoneal administration of glucose (1 g/kg body weight) or insulin (0.75 U/kg body weight). Blood glucose was measured with an Ascenzia Breeze 2 glucometer (Bayer), and blood insulin was measured by enzyme-linked immunosorbent assay (ELISA) (Luminex 200, Millipore).

Hyperinsulinemic-euglycemic clamp studies. The clamp studies were performed at the Pennsylvania State Diabetes and Obesity Mouse Phenotyping Center. Whole-body fat and lean mass were noninvasively measured using ^{1}H-MRS (Echo Medical Systems). Following an overnight fast, a 2-h hyperinsulinemic-euglycemic clamp study was conducted in conscious mice with a primed and continuous infusion of human insulin (150 mU/kg body weight priming followed by 2.5 mU/kg/min; Humulin, Eli Lilly), and 20% glucose was infused at variable rates to maintain euglycemia (23). Whole-body glucose turnover was assessed with a continuous infusion of [3-^{3}H]glucose (PerkinElmer), and 2-deoxy-D-[1-^{14}C]glucose (PerkinElmer) was administered as a bolus (10 μCi) at 75 min after the start of the clamp study to measure insulin-stimulated glucose uptake in individual organs. At the end of the clamp study, mice were anesthetized and tissues were taken for biochemical analysis (23).

Analysis of tissue sections. Upon necropsy, gross organ analysis was performed. In addition, samples of liver, spleen, thymus, lymph nodes, kidney, heart, pancreas, fat, and muscle were removed. Histology was performed using tissue fixed in 10% formalin for 24 h, dehydrated, and embedded in paraffin. Sections (7 μm) were cut, stained using hematoxylin and eosin (American Master Tech Scientific), and examined by a board-certified veterinary pathologist.

Insulin treatment and immunoblot analysis. For insulin response *in vivo*, mice were fasted overnight. Mice were injected with 1.5 U of insulin, and tissues were harvested 30 min later. Tissues were homogenized in Triton lysis buffer (20 mM Tris [pH 7.4], 1% Triton X-100, 10% glycerol, 137 mM NaCl, 2 mM EDTA, 25 mM β-glycerophosphate, 1 mM sodium orthovanadate, 1 mM phenylmethylsulfonyl fluoride, and 10 μg/ml of aprotinin and leupeptin). Tissue extracts (50 μg) were examined by immunoblot analysis using antibodies to Akt, phospho-Ser473 Akt, and phospho-Thr172 AMPKα (Cell Signaling). Flag-sestrin 2 was detected with anti-Flag antibody (Sigma).

Cytokine analysis. The amount of cytokines in plasma was measured by multiplexed ELISA by using a Luminex 200 machine (Millipore) and serum mouse adipokine, adiponectin, and cytokine kits (Millipore).

Blood lipid analysis. The amount of triglyceride was measured using the CardioCheck meter and triglyceride strips (Polymer Technology Systems, Indianapolis, IN).

RNA preparation and analysis. RNA was prepared from tissues collected in RNAlater (Ambion) and snap-frozen in liquid nitrogen. Total RNA was prepared with RNeasy kits (Qiagen) by following the manufacturer's instructions. The purified RNA was subjected to an additional DNase treatment (Ambion) to ensure the removal of contaminating genomic DNA prior to final column purification. The relative expression of mRNA was examined by quantitative PCR analysis. cDNA was prepared using Superscript III (Invitrogen) with random hexamers and 0.5 μg to 1 μg of RNA per tissue. Quantitative real-time PCR was performed on a Bio-Rad iCycler using Sybr green master mix (Bio-Rad). The primer sequences for the murine genes were as follows: *Gapdh* (5′-CTTCA CCACCATGGAGAAGGC-3′, 5′-GGCATGGACTGTGGTCAT-3′), *p53* (5′-TGAAACGCCGACCTATCCTTA-3′, 5′-GGCACAAACACGAACCTC AAA-3′), *Mdm2* (5′-TGACACCAGAGCTTAGTCCTG-3′, 5′-GCGTCTCG TAACGAATAAGGC-3′), *Zfp385a* (5′-ACATTGAGCACCGCTATGTCT-3′, 5′-CTCTCTTGGATGAGGGTCTGATA-3′), *Sesn1* (5′-GTGGACCCAG AACGAGATGACGTGGC-3′, 5′-GACACTGTGGAAGGCAGCTATGTG C-3′), *Sesn2* (5′-TCCGAGTGCCATTCCGAGAT-3′, 5′-TCCGGGTGTAG ACCCATCAC-3′), *Sesn3* (5′-GCGAGGAGAAGAACATTTGCC-3′, 5′-CCA AACATACAGTGAACATAGT-3′), *Sco2* (5′-GTGGACCCAGAACGAGAT GACGTGGC-3′, 5′-GACACTGTGGAAGGCAGCTATGTGC-3′), and *Tigar* (5′-CAAGCAGCGGCCGCCGGGCAGTTTCTG-3′, 5′-CTCCTGGCAACGA GCATCTGAGGTCAC-3′). All samples were examined in triplicate, and values were normalized for baseline expression and for expression of *Gapdh*. Calculations of values were made using the $\Delta\Delta CT$ method. Statistical significance was calculated using threshold cycle (C_T) values.

Tissue culture. Primary murine embryo fibroblasts (MEFs) were prepared from E14 wild-type and $p53^{S18A}$ embryos (11). The MEFs were cultured in Dulbecco's modified Eagle's medium supplemented with 10% fetal bovine serum (Invitrogen). Early-passage MEFs were at passage 2 and later-passage MEFs were passage 4 ($p53^{S18A}$ MEFs lose viability at this time). For insulin response analysis, cells were starved 15 to 18 h in Dulbecco's phosphate-buffered saline (D-PBS) with calcium, magnesium, and 5 mM glucose. Cells were treated with insulin (10 nM) and harvested at the indicated time points. For *N*-acetyl cysteine (NAC) treatment, cells were thawed and fed with medium containing 0.5 mM NAC (Sigma) for four passages and examined for insulin response. For hydrogen peroxide treatment, cells were plated (12,000 onto a 6-well plate) and incubated with hydrogen peroxide (0, 44, 88, and 176 μM) and harvested at 24 h. Relative viability was determined by the trypan blue staining method.

Reactive oxygen species. For the detection of intracellular ROS levels, MEFs were incubated with 10 μg/ml 2′,7′-dichlorofluorescein diacetate (DCF; Sigma) in PBS supplemented with 5 mM glucose (20 min, 37°C), washed twice with PBS-glucose, suspended in Dulbecco's modified Eagle's medium (5 mM glucose, no phenol red), incubated at 37°C (20 min), and examined by flow cytometry (28). For sestrin expression, lentivirus expressing Sesn2 and green fluorescent protein (GFP) (pVL-Sesn2F and pVL-GFP [9]) were produced by the University of Massachusetts Medical School vector core. Cells (0.5×10^6) were infected with 10 μl concentrated virus. Transduction was confirmed by GFP and Flag-sesn 2 expression.

Data analysis. To calculate statistical changes in metabolic parameters, statistically significant differences ($P < 0.05$) between groups were examined using the two-tailed Student *t* test. Microsoft Excel was used for statistical calculations.

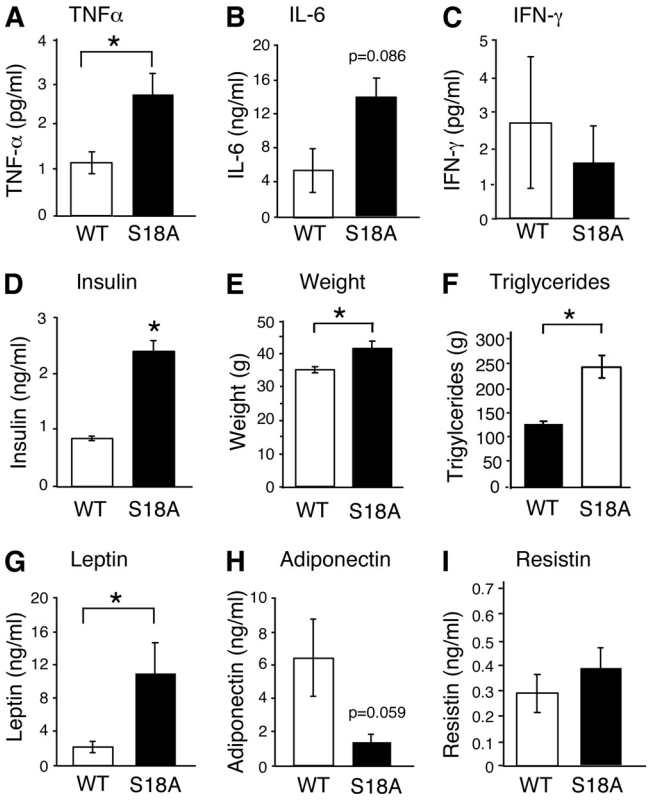

FIG. 2. Analysis of cytokines and metabolic parameters. Wild-type (WT) and $p53^{S18A}$ (S18A) mice were maintained on a standard chow diet. Experiments were performed on 6- to 7-month-old animals. (A to C) WT and $p53^{S18A}$ mice were fasted overnight, and the concentrations of TNF-α, IL-6, and IFN-γ in blood were measured (means ± SEM; $n = 6$ animals). (D) Insulin measurement in mice fasted overnight (means ± SEM; $n = 9$). (E) Body weight was measured at 6 months (means ± SEM; $n = 15$). (F) Concentration of triglyceride in the blood of WT and $p53^{S18A}$ mice was measured (means ± standard deviation [SD]; $n = 3$). (G to I) The concentrations of the adipokines leptin, adiponectin, and resistin in the blood of mice fasted overnight were measured (means ± SEM; $n = 7$). Statistically significant differences between WT and $p53^{S18A}$ mice are indicated (*, $P < 0.05$).

RESULTS

Expression of antioxidant sestrins and metabolic genes mediated by p53 Ser18. Increased levels of reactive oxygen species (ROS) have been proposed as the major cause of pathologies in A-T patients and *Atm* mutant mice (47). A-T patients present with increased lipid peroxidation and oxidative DNA damage (37), and tissues from $Atm^{-/-}$ mice exhibit ROS-induced damage (20). Increased ROS production (e.g., as a by-product of mitochondrial oxidative phosphorylation) can contribute to inflammation and insulin resistance (14, 34, 40). p53 has been implicated in the regulation of oxidative stress. We therefore examined whether a mutation of the ATM phosphorylation site on p53 caused increased ROS accumulation. We found that primary fibroblasts prepared from $p53^{S18A}$ mice generated increased amounts of ROS compared with ROS levels in wild-type fibroblasts (Fig. 1A). In contrast, treatment of wild-type and $p53^{S18A}$ fibroblasts with H_2O_2 (a physiological form of ROS) caused a similar decrease in viability (Fig. 1B). The increased ROS production may therefore account for pre-

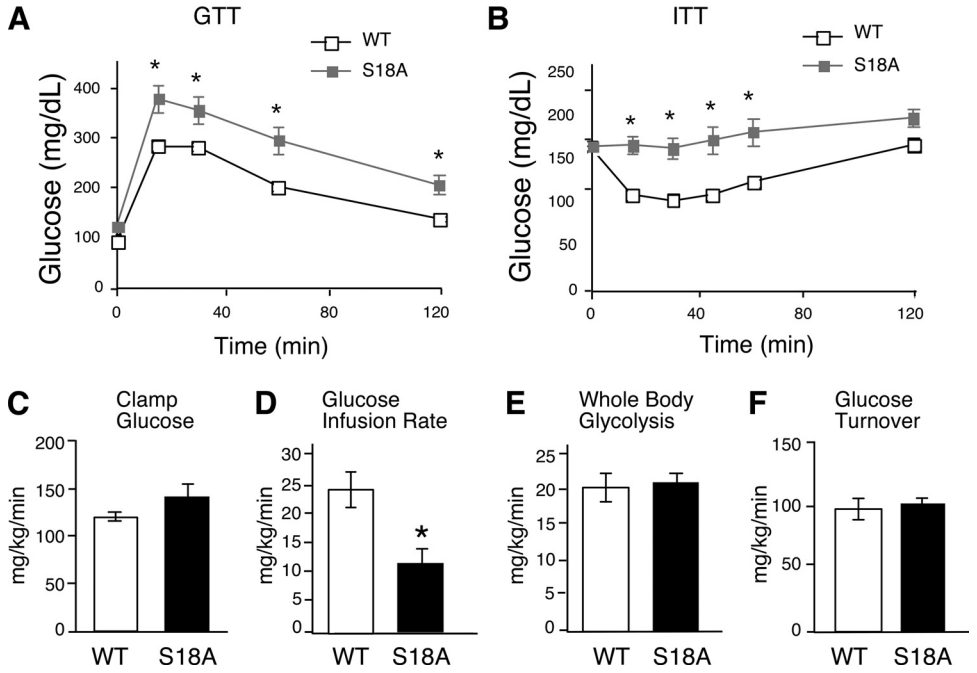

FIG. 3. Insulin resistance in $p53^{S18A}$ mice. Wild-type (WT) and $p53^{S18A}$ (S18A) mice were maintained on a standard chow diet. Experiments were performed on 6- to 7-month-old animals. (A) Glucose tolerance test (GTT). Mice fasted overnight were treated with glucose (1 g/kg) by intraperitoneal injection. Blood glucose concentration was measured at the indicated times (means ± SEM; $n = 15$ to 20). (B) Insulin tolerance test (ITT). Mice fed *ad libitum* were treated with insulin (0.75 U/kg) by intraperitoneal injection. Blood glucose levels were measured at the indicated times (means ± SEM; $n = 15$ to 20). (C to F) Hyperinsulinemia-euglycemic clamp analysis (means ± SEM; $n = 7$ or 8). (C) Blood glucose concentration during the hyperinsulinemia-euglycemic clamp analysis; (D) steady-state glucose infusion rates to maintain euglycemia during the clamp; (E) whole-body glycolysis; (F) insulin-stimulated whole-body glucose turnover. Statistically significant differences are indicated (*, $P < 0.05$).

vious reports that $p53^{S18A}$ fibroblasts, like $Atm^{-/-}$ fibroblasts (49), exhibit decreased growth and accelerated senescence compared to wild-type fibroblasts (1). It has been reported that p53 can regulate the expression of the synthesis of the cytochrome *c* oxidase 2 gene (*Sco2*), which is required for mitochondrial respiration (29). We examined *Sco2* expression and found no difference between $p53^{S18A}$ and wild-type fibroblasts (Fig. 1C). There was no significant difference in *p53* expression between $p53^{S18A}$ and wild-type fibroblasts (data not shown). Thus, increased ROS levels in $p53^{S18A}$ fibroblasts may not be due to defective mitochondrial function.

Cellular antioxidants represent an important mechanism of ROS regulation. Indeed, p53 can regulate the expression of antioxidants (8, 38). Thus, the increased ROS levels in $p53^{S18A}$ fibroblasts may be caused by decreased antioxidant gene expression (38). To test this hypothesis, we examined the expression of *Sestrins*, p53 target genes that modulate the function of peroxiredoxin (9). The expression of *Sestrin 1*, *2*, and *3* was significantly reduced in $p53^{S18A}$ fibroblasts compared to that in wild-type fibroblasts (Fig. 1C). These defects in S*estrin* gene expression may contribute to the increased ROS levels detected in $p53^{S18A}$ fibroblasts (Fig. 1A). Similarly, S*estrin* gene expression was significantly reduced in the livers of $p53^{S18A}$ mice compared to that in wild-type mice (Fig. 1D). In contrast, *Tigar* expression was not significantly reduced in the livers of $p53^{S18A}$ mice (Fig. 1D). This further supports that defects in homeostasis are not due to mitochondrial respiration abnormalities. The decrease in *Sestrin* expression in the adipose tissue and muscle of $p53^{S18A}$ mice was not significant (Fig. 1E). We examined $Atm^{-/+}$ mice that were insulin resistant (data not shown) and observed a significant decrease in *Sestrin 2* and *Sestrin 3* expression (Fig. 1F), suggesting that this activation of p53 is mediated by ATM phosphorylation in the liver.

Increased metabolic stress in p53 Ser18 phosphorylation-deficient animals. The mutation of ATM leads to increased inflammation, including the expression of tumor necrosis factor alpha (TNF-α), interleukin 6 (IL-6), and C-reactive peptide (47). These cytokines are implicated in insulin resistance (6). We examined cytokine expression in young wild-type and $p53^{S18A}$ animals and observed no difference (data not shown). We also examined cytokine expression in 6-month-old $p53^{S18A}$ animals. We found a significant increase in the circulating levels of TNF-α in $p53^{S18A}$ mice compared with levels in wild-type mice (Fig. 2A). Although not significant, IL-6 levels in the blood were also elevated (Fig. 2B), and gamma interferon (IFN-γ) levels were reduced (Fig. 2C).

The finding that $p53^{S18A}$ mice have reduced antioxidant gene expression (e.g., *Sestrins*) and increased expression of inflammatory cytokines (e.g., TNF-α) suggests that these mice may exhibit metabolic stress. To test this hypothesis, we compared various metabolic parameters in wild-type and $p53^{S18A}$ mice. Insulin levels were significantly increased in $p53^{S18A}$ animals (Fig. 2D). There was a modest but significant ($P < 0.05$) increase in body weight in the 24-week-old $p53^{S18A}$ mice compared to that in wild-type mice (Fig. 2E), with the difference attributed mainly to an increased weight of fat pads (data not

shown). The fasting blood triglyceride was increased in $p53^{S18A}$ mice compared with that in wild-type mice (Fig. 2F). Studies of adipokines demonstrated a significant increase in blood leptin levels (Fig. 2G). These data are consistent with the observation that the levels of circulating leptin are proportional to the total amount of body fat, as leptin is primarily made in adipocytes (13). There was also a decrease in adiponectin levels; however, it was of borderline significance ($P = 0.059$) (Fig. 2H). Resistin levels were not different (Fig. 2I). Furthermore, the pancreatic islets of $p53^{S18A}$ mice exhibited hypertrophy compared with those of wild-type mice (unpublished observation).

Defective glucose homeostasis and insulin resistance in $p53^{S18A}$ mice. The observation of decreased antioxidant defense, increased markers of inflammation and metabolic stress, and deregulation of genes important for metabolic control suggested that p53 Ser18 could be a good candidate for mediating glucose homeostasis mediated by ATM. We analyzed glucose metabolism of $p53^{S18A}$ animals by performing a glucose tolerance test and insulin tolerance test on tumor-free animals (Fig. 3). Wild-type and $p53^{S18A}$ mice were maintained on a chow diet. Baseline glucose tolerance and insulin tolerance tests were performed at 3 months, and no significant difference was observed (data not shown). However, we hypothesized that the effects of antioxidant loss could exhibit a time-dependent effect. Thus, we examined glucose homeostasis in animals at 6 months of age. $p53^{S18A}$ mice exhibited glucose intolerance (Fig. 3A) and insulin resistance (Fig. 3B) at 6 months of age. Together, these data indicate that adult $p53^{S18A}$ mice are insulin resistant. To test this hypothesis, we performed a hyperinsulinemic-euglycemic clamp study to examine insulin sensitivity in conscious mice.

During the euglycemic clamp study, plasma glucose levels were similarly maintained at ~130 mg/dl in both groups of mice (Fig. 3C). The steady-state glucose infusion rate during the clamp study was significantly reduced in $p53^{S18A}$ mice compared to that in wild-type mice (Fig. 3D). Insulin-stimulated whole-body glucose turnover and glycolysis were not altered in $p53^{S18A}$ mice (Fig. 3E and F). In contrast, insulin-stimulated whole-body glycogen synthesis was reduced in $p53^{S18A}$ mice compared to that in wild-type mice (Fig. 4A). Levels of basal hepatic glucose production (HGP) by wild-type and $p53^{S18A}$ mice were similar (Fig. 4B). However, insulin failed to suppress HGP during the clamp study in $p53^{S18A}$ mice, indicating severe hepatic insulin resistance in these mice (Fig. 4B). To obtain biochemical evidence for selective insulin resistance in $p53^{S18A}$ mice, we examined insulin-stimulated activation of Akt in liver (Fig. 4C). We found that insulin caused Akt activation in the muscles of both wild-type and $p53^{S18A}$ mice. In contrast, insulin caused Akt activation in the livers of wild-type mice but not in $p53^{S18A}$ mice. Importantly, the animals used in these experiments were determined to be tumor free. Together, these data demonstrate that $p53^{S18A}$ mice exhibit hepatic insulin resistance.

The increased production of ROS and loss of antioxidant gene expression suggested that reactive oxygen species could be mediating the metabolic effects observed in the $p53^{S18A}$ animals. In order to first examine this, we tested whether sestrin expression could reduce the levels of ROS observed in $p53^{S18A}$ MEFs (Fig. 1A). We generated $p53^{S18A}$ MEFs expressing sestrin 2 and determined that increased levels of sestrin 2

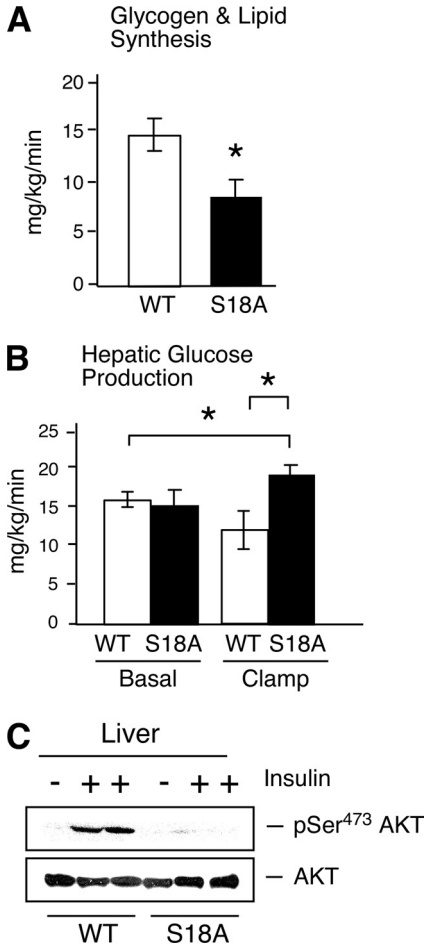

FIG. 4. $p53^{S18A}$ mice exhibit hepatic insulin resistance. (A and B) Wild-type (WT) and $p53^{S18A}$ (S18A) mice were maintained on a standard chow diet. The data presented are the means ± SEM ($n = 7$ or 8). Statistically significant differences are indicated (*, $P < 0.05$). (A) Whole-body glycogen synthesis; (B) basal hepatic glucose production (HGP) (left) and insulin-stimulated HGP during the hyperinsulinemia-euglycemic clamp analysis (right). (C) Extracts prepared from the liver of WT and $p53^{S18A}$ mice were examined by immunoblot analysis using antibodies to Akt and pSer473 Akt. The mice were fasted overnight and treated without and with insulin (1.5 U/kg body mass) by intraperitoneal injection (30 min).

decreased the levels of ROS in $p53^{S18A}$ MEFs (Fig. 5A). We observed decreased Akt phosphorylation in $p53^{S18A}$ MEFs at passage 4 (Fig. 5B). However, the examination of the phosphorylation of Thr172 of AMPKα showed no difference (data not shown). The $p53^{S18A}$ cells exhibit morphological characteristics of senescence and exhibit greatly reduced viability at increasing passages (1). The treatment of the cells with the antioxidant NAC restored insulin signaling and improved the morphology of the cells (Fig. 5C). We next tested whether increased ROS levels are affecting the glucose intolerance observed in the $p53^{S18A}$ animals. We placed wild-type and $p53^{S18A}$ animals on a diet supplemented with 1.5% BHA and compared results to those for animals whose diet did not contain BHA. BHA treatment of the wild-type animals had no effect on glucose homeostasis (Fig. 5D). However, dietary supplementation with BHA significantly reduced the insulin sen-

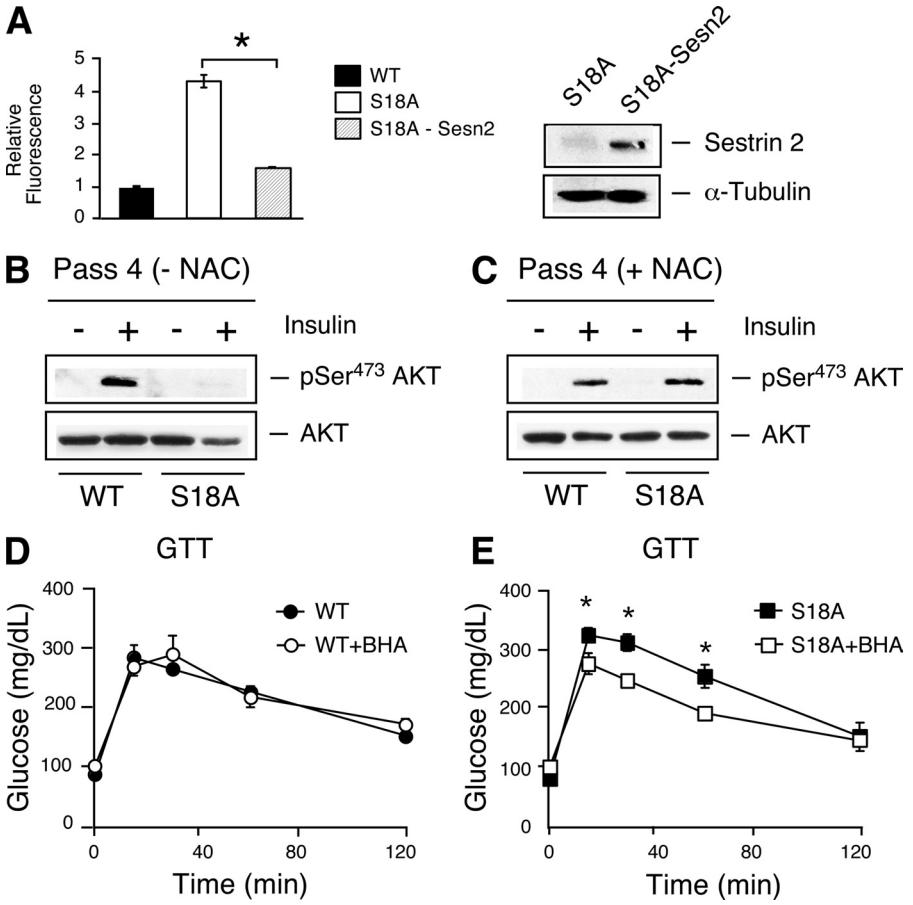

FIG. 5. Role of increased ROS levels in metabolic defects in $p53^{S18A}$ mice. (A) Reduction of ROS levels by the expression of sestrin 2. Left, the amount of reactive oxygen species (ROS) in $p53^{S18A}$ MEFs was examined by DCF staining and analysis by flow cytometry and compared to that in wild-type cells. Data are presented as relative fluorescence (means ± SEM; $n = 5$). Right, Western analysis of the cells used in the experiment shown in the left panel, indicating expression of sestrin 2. (B and C) Insulin signaling is improved with NAC treatment. Passage 4 cells that were untreated (B) or treated with 0.5 mM NAC (C) were starved for 18 h and treated with 10 nM insulin. Akt and pSer473 Akt were examined by immunoblot. (D and E) Wild-type (WT) and $p53^{S18A}$ (S18A) mice were maintained on a standard chow diet or a diet including 1.5% BHA for approximately 4 weeks (at 6 months of age). Glucose tolerance test (GTT) on wild-type mice (D) and $p53^{S18A}$ mice (E). Mice fasted overnight were treated with glucose (1 g/kg) by intraperitoneal injection. The blood glucose concentration was measured at the indicated times (means ± SEM; $n = 15$ to 20). Statistically significant differences are indicated (*, $P < 0.05$).

sitivity in $p53^{S18A}$ animals (Fig. 5E) to a level where the GTT results exhibited no difference compared to results for wild-type animals. These data indicate that deregulated ROS contributes to the imbalance in glucose homeostasis in $p53^{S18A}$ animals.

DISCUSSION

ATM is activated by a number of stresses that have a direct impact on metabolism. A number of these cellular stresses, including atherosclerosis, trauma, hypoxia, and infections, are associated with p53 activation and p53 Ser18 phosphorylation (12, 30, 32, 39, 44, 50, 51). A-T patients exhibit an increased risk of insulin resistance and type 2 diabetes (3). In addition, loss of *Atm* has been implicated in metabolic disease (42). *Atm* mutant animals have been shown to be glucose intolerant and insulin resistant. Our analysis demonstrates that the ATM phosphorylation site on murine p53 (Ser18) exerts a protective role in maintaining glucose homeostasis. p53 Ser18-deficient animals exhibited glucose intolerance and insulin resistance. Although multiple factors can contribute to the development of insulin resistance, including oxidative stress, inflammation, and obesity (6), oxidative stress has been proposed to be the major contributor to pathology in A-T patients (4, 15, 20). One important substrate for ATM is the p53 tumor suppressor. We observed that cells from p53 Ser18-defective mice ($p53^{S18A}$ mice) exhibited increased levels of reactive oxygen species (ROS). In addition, we determined that the p53 Ser18 phosphorylation site is required for p53-dependent antioxidant gene expression (e.g., *Sestrin*) in MEFs and in the liver (Fig. 1). Although we did not observe statistically significant changes in other mediators of mitochondrial respiration, further examination needs to be made to test whether the changes we observed in TIGAR expression have an effect on homeostasis.

Another clinical observation in A-T patients and *Atm* mutant mice is increased metabolic stress, such as increased proinflammatory cytokine expression. We observed significantly increased plasma levels of the proinflammatory cytokine TNF-α

in $p53^{S18A}$ animals. Analysis of other metabolic parameters indicated deregulated metabolism in these animals. For instance, the $p53^{S18A}$ animals had increased body weight and elevated basal serum insulin levels compared to those in wild-type animals. We propose that these effects are indirect effects of the changes to the expression of the metabolic genes regulated by p53 Ser18. The role of sestrins in oxidative stress provides data that they may have a substantial role in the defects observed in the $p53^{S18A}$ animals. Furthermore, we observed insulin resistance in older animals, suggesting that the pathologies that lead to defects in glucose homeostasis accumulate with time. The role of oxidative stress in aging is well established (2, 17). Importantly, hydrogen peroxide, whose levels are regulated indirectly by the sestrin gene family, is also implicated in aging (16). Our data are in agreement with the model that accumulated oxidative damage affects glucose homeostasis.

Through clamp analysis, we have identified the liver as the primary organ of insulin resistance. We also demonstrated reduced Akt activation in the liver, following insulin stimulation. Interestingly, sestrin expression was also significantly reduced in the liver. This suggests that a loss of sestrin expression leads to increased oxidative stress in the liver, which disrupts insulin sensitivity. In support of this model, treatment of $p53^{S18A}$ mice leads to restored glucose tolerance, whereas wild-type mice remain unchanged. This demonstrates a specific improvement in the $p53^{S18A}$ mice due to decreased levels of ROS *in vivo*. In addition, studies in MEFs indicate that NAC treatment restores insulin sensitivity. This has been observed in *Atm*-deficient MEFs as well (18). AMPKα has been shown to phosphorylate p53 Ser18 *in vitro* (19); however, a role in AMPK-mediated response to glucose is not clear (26). In addition, AMPKα-deficient mice develop muscle insulin resistance (45), which is not observed in $p53^{S18A}$ mice. Thus, although there may be additional kinases that regulate p53 Ser18 *in vivo*, there is a clear connection with *Atm* deficiency, increased oxidative stress, and insulin resistance. Together, these data indicate that the ATM-p53 pathway causes tissue-specific changes in gene expression that function collectively to maintain insulin sensitivity and glucose homeostasis. Thus, mice with a targeted mutation in the ATM phosphorylation site on p53 (Ser18) exhibit insulin resistance. Moreover, disruption of this pathway in A-T patients may contribute to deregulation of metabolism. These data establish that the modulation of the ATM-p53 pathway is an important mechanism that contributes to normal glucose homeostasis.

ACKNOWLEDGMENTS

We thank Roger Davis for critical reading of the manuscript; Guadalupe Sabio, Anja Jaeschke, and other members of the Davis laboratory for helpful discussions and invaluable technical assistance; David Garlick for histology analysis; Ceren Acer, Chrisitine Delaney, and Charissa Cottonham for assistance with real-time PCR analysis; Punita Shroff for help with hydrogen peroxide experiments; and Andrei Budanov for kindly providing plasmids.

These studies were supported by a Pilot & Feasibility grant from the UMass Diabetes Endocrinology Research Center (NIH P30 DK32520 to H.K.S.), Worcester Foundation for Biomedical Research (to H.S.K.), and by grants from the NIH (DK80756 to J.K.K.) and the American Diabetes Association (7-07-RA-80 to J.K.K.). Core resources supported by the Diabetes Endocrinology Research Center grant (DK32520) were also used. Hayla K. Sluss and Jason K. Kim are members of the UMass DERC (DK32520). Part of this study was performed at the Penn State Diabetes & Obesity Mouse Phenotyping Center (supported by the Pennsylvania Department of Health and Tobacco Settlement Funds).

We declare that we have no conflicts of interest.

REFERENCES

1. **Armata, H. L., D. S. Garlick, and H. K. Sluss.** 2007. The ataxia telangiectasia-mutated target site Ser18 is required for p53-mediated tumor suppression. Cancer Res. **67:**11696–11703.
2. **Balaban, R. S., S. Nemoto, and T. Finkel.** 2005. Mitochondria, oxidants, and aging. Cell **120:**483–495.
3. **Bar, R. S., W. R. Levis, M. M. Rechler, L. C. Harrison, C. Siebert, J. Podskalny, J. Roth, and M. Muggeo.** 1978. Extreme insulin resistance in ataxia telangiectasia: defect in affinity of insulin receptors. N. Engl. J. Med. **298:**1164–1171.
4. **Barlow, C., P. A. Dennery, M. K. Shigenaga, M. A. Smith, J. D. Morrow, L. J. Roberts III, A. Wynshaw-Boris, and R. L. Levine.** 1999. Loss of the ataxia-telangiectasia gene product causes oxidative damage in target organs. Proc. Natl. Acad. Sci. U. S. A. **96:**9915–9919.
5. **Barlow, C., S. Hirotsune, R. Paylor, M. Liyanage, M. Eckhaus, F. Collins, Y. Shiloh, J. N. Crawley, T. Ried, D. Tagle, and A. Wynshaw-Boris.** 1996. Atm-deficient mice: a paradigm of ataxia telangiectasia. Cell **86:**159–171.
6. **Bastard, J. P., M. Maachi, C. Lagathu, M. J. Kim, M. Caron, H. Vidal, J. Capeau, and B. Feve.** 2006. Recent advances in the relationship between obesity, inflammation, and insulin resistance. Eur. Cytokine Netw. **17:**4–12.
7. **Bensaad, K., and K. H. Vousden.** 2007. p53: new roles in metabolism. Trends Cell Biol. **17:**286–291.
8. **Bensaad, K., and K. H. Vousden.** 2005. Savior and slayer: the two faces of p53. Nat. Med. **11:**1278–1279.
9. **Budanov, A. V., A. A. Sablina, E. Feinstein, E. V. Koonin, and P. M. Chumakov.** 2004. Regeneration of peroxiredoxins by p53-regulated sestrins, homologs of bacterial AhpD. Science **304:**596–600.
10. **Chao, C., S. Saito, C. W. Anderson, E. Appella, and Y. Xu.** 2000. Phosphorylation of murine p53 at ser-18 regulates the p53 responses to DNA damage. Proc. Natl. Acad. Sci. U. S. A. **97:**11936–11941.
11. **Donehower, L. A., M. Harvey, B. L. Slagle, M. J. McArthur, C. A. Montgomery, Jr., J. S. Butel, and A. Bradley.** 1992. Mice deficient for p53 are developmentally normal but susceptible to spontaneous tumours. Nature **356:**215–221.
12. **Eizenberg, O., A. Faber-Elman, E. Gottlieb, M. Oren, V. Rotter, and M. Schwartz.** 1995. Direct involvement of p53 in programmed cell death of oligodendrocytes. EMBO J. **14:**1136–1144.
13. **Frederich, R. C., A. Hamann, S. Anderson, B. Lollmann, B. B. Lowell, and J. S. Flier.** 1995. Leptin levels reflect body lipid content in mice: evidence for diet-induced resistance to leptin action. Nat. Med. **1:**1311–1314.
14. **Fridlyand, L. E., and L. H. Philipson.** 2006. Reactive species and early manifestation of insulin resistance in type 2 diabetes. Diabetes Obes. Metab. **8:**136–145.
15. **Gatei, M., D. Shkedy, K. K. Khanna, T. Uziel, Y. Shiloh, T. K. Pandita, M. F. Lavin, and G. Rotman.** 2001. Ataxia-telangiectasia: chronic activation of damage-responsive functions is reduced by alpha-lipoic acid. Oncogene **20:**289–294.
16. **Giorgio, M., M. Trinei, E. Migliaccio, and P. G. Pelicci.** 2007. Hydrogen peroxide: a metabolic by-product or a common mediator of ageing signals? Nat. Rev. Mol. Cell Biol. **8:**722–728.
17. **Golden, T. R., D. A. Hinerfeld, and S. Melov.** 2002. Oxidative stress and aging: beyond correlation. Aging Cell **1:**117–123.
18. **Ito, K., K. Takubo, F. Arai, H. Satoh, S. Matsuoka, M. Ohmura, K. Naka, M. Azuma, K. Miyamoto, K. Hosokawa, Y. Ikeda, T. W. Mak, T. Suda, and A. Hirao.** 2007. Regulation of reactive oxygen species by Atm is essential for proper response to DNA double-strand breaks in lymphocytes. J. Immunol. **178:**103–110.
19. **Jones, R. G., D. R. Plas, S. Kubek, M. Buzzai, J. Mu, Y. Xu, M. J. Birnbaum, and C. B. Thompson.** 2005. AMP-activated protein kinase induces a p53-dependent metabolic checkpoint. Mol. Cell **18:**283–293.
20. **Kamsler, A., D. Daily, A. Hochman, N. Stern, Y. Shiloh, G. Rotman, and A. Barzilai.** 2001. Increased oxidative stress in ataxia telangiectasia evidenced by alterations in redox state of brains from Atm-deficient mice. Cancer Res. **61:**1849–1854.
21. **Kastan, M. B., and D. S. Lim.** 2000. The many substrates and functions of ATM. Nat. Rev. Mol. Cell Biol. **1:**179–186.
22. **Kawagishi, H., T. Wakoh, H. Uno, M. Maruyama, A. Moriya, S. Morikawa, H. Okano, C. J. Sherr, M. Takagi, and M. Sugimoto.** 2008. Hzf regulates adipogenesis through translational control of C/EBPalpha. EMBO J. **27:**1481–1490.
23. **Kim, H. J., T. Higashimori, S. Y. Park, H. Choi, J. Dong, Y. J. Kim, H. L. Noh, Y. R. Cho, G. Cline, Y. B. Kim, and J. K. Kim.** 2004. Differential effects of interleukin-6 and -10 on skeletal muscle and liver insulin action in vivo. Diabetes **53:**1060–1067.
24. **Kondoh, H., M. E. Lleonart, J. Gil, J. Wang, P. Degan, G. Peters, D.**

Martinez, A. Carnero, and D. Beach. 2005. Glycolytic enzymes can modulate cellular life span. Cancer Res. **65:**177–185.
25. **Lavin, M. F.** 2008. Ataxia-telangiectasia: from a rare disorder to a paradigm for cell signaling and cancer. Nat. Rev. Mol. Cell Biol. **9:**759–769.
26. **Lee, C. H., K. Inoki, M. Karbowniczek, E. Petroulakis, N. Sonenberg, E. P. Henske, and K. L. Guan.** 2007. Constitutive mTOR activation in TSC mutants sensitizes cells to energy starvation and genomic damage via p53. EMBO J. **26:**4812–4823.
27. **Liu, B., Y. Chen, and D. K. St. Clair.** 2008. ROS and p53: a versatile partnership. Free Radic. Biol. Med. **44:**1529–1535.
28. **Matheu, A., A. Maraver, P. Klatt, I. Flores, I. Garcia-Cao, C. Borras, J. M. Flores, J. Vina, M. A. Blasco, and M. Serrano.** 2007. Delayed ageing through damage protection by the Arf/p53 pathway. Nature **448:**375–379.
29. **Matoba, S., J. G. Kang, W. D. Patino, A. Wragg, M. Boehm, O. Gavrilova, P. J. Hurley, F. Bunz, and P. M. Hwang.** 2006. p53 regulates mitochondrial respiration. Science **312:**1650–1653.
30. **Mercer, J., N. Figg, V. Stoneman, D. Braganza, and M. R. Bennett.** 2005. Endogenous p53 protects vascular smooth muscle cells from apoptosis and reduces atherosclerosis in ApoE knockout mice. Circ. Res. **96:**667–674.
31. **Minamino, T., M. Orimo, I. Shimizu, T. Kunieda, M. Yokoyama, T. Ito, A. Nojima, A. Nabetani, Y. Oike, H. Matsubara, F. Ishikawa, and I. Komuro.** 2009. A crucial role for adipose tissue p53 in the regulation of insulin resistance. Nat. Med. **15:**1082–1087.
32. **Moon, C., S. Kim, M. Wie, H. Kim, J. Cheong, J. Park, Y. Jee, N. Tanuma, Y. Matsumoto, and T. Shin.** 2000. Increased expression of p53 and Bax in the spinal cords of rats with experimental autoimmune encephalomyelitis. Neurosci. Lett. **289:**41–44.
33. **Mora, A., K. Sakamoto, E. J. McManus, and D. R. Alessi.** 2005. Role of the PDK1-PKB-GSK3 pathway in regulating glycogen synthase and glucose uptake in the heart. FEBS Lett. **579:**3632–3638.
34. **Newsholme, P., E. P. Haber, S. M. Hirabara, E. L. Rebelato, J. Procopio, D. Morgan, H. C. Oliveira-Emilio, A. R. Carpinelli, and R. Curi.** 2007. Diabetes associated cell stress and dysfunction: role of mitochondrial and non-mitochondrial ROS production and activity. J. Physiol. **583:**9–24.
35. **Pani, G., O. R. Koch, and T. Galeotti.** 2009. The p53-p66shc-manganese superoxide dismutase (MnSOD) network: a mitochondrial intrigue to generate reactive oxygen species. Int. J. Biochem. Cell Biol. **41:**1002–1005.
36. **Polyak, K., Y. Xia, J. L. Zweier, K. W. Kinzler, and B. Vogelstein.** 1997. A model for p53-induced apoptosis. Nature **389:**300–305.
37. **Reichenbach, J., R. Schubert, D. Schindler, K. Muller, H. Bohles, and S. Zielen.** 2002. Elevated oxidative stress in patients with ataxia telangiectasia. Antioxid. Redox Signal. **4:**465–469.
38. **Sablina, A. A., A. V. Budanov, G. V. Ilyinskaya, L. S. Agapova, J. E. Kravchenko, and P. M. Chumakov.** 2005. The antioxidant function of the p53 tumor suppressor. Nat. Med. **11:**1306–1313.
39. **Sakhi, S., A. Bruce, N. Sun, G. Tocco, M. Baudry, and S. S. Schreiber.** 1994. p53 induction is associated with neuronal damage in the central nervous system. Proc. Natl. Acad. Sci. U. S. A. **91:**7525–7529.
40. **Savage, D. B., K. F. Petersen, and G. I. Shulman.** 2005. Mechanisms of insulin resistance in humans and possible links with inflammation. Hypertension **45:**828–833.
41. **Schwartzenberg-Bar-Yoseph, F., M. Armoni, and E. Karnieli.** 2004. The tumor suppressor p53 down-regulates glucose transporters GLUT1 and GLUT4 gene expression. Cancer Res. **64:**2627–2633.
42. **Shoelson, S. E.** 2006. Banking on ATM as a new target in metabolic syndrome. Cell Metab. **4:**337–338.
43. **Sluss, H. K., H. Armata, J. Gallant, and S. N. Jones.** 2004. Phosphorylation of serine 18 regulates distinct p53 functions in mice. Mol. Cell. Biol. **24:**976–984.
44. **van Vlijmen, B. J., G. Gerritsen, A. L. Franken, L. S. Boesten, M. M. Kockx, M. J. Gijbels, M. P. Vierboom, M. van Eck, B. van De Water, T. J. van Berkel, and L. M. Havekes.** 2001. Macrophage p53 deficiency leads to enhanced atherosclerosis in APOE*3-Leiden transgenic mice. Circ. Res. **88:**780–786.
45. **Viollet, B., F. Andreelli, S. B. Jorgensen, C. Perrin, D. Flamez, J. Mu, J. F. Wojtaszewski, F. C. Schuit, M. Birnbaum, E. Richter, R. Burcelin, and S. Vaulont.** 2003. Physiological role of AMP-activated protein kinase (AMPK): insights from knockout mouse models. Biochem. Soc. Trans. **31:**216–219.
46. **Vousden, K. H., and D. P. Lane.** 2007. p53 in health and disease. Nat. Rev. Mol. Cell Biol. **8:**275–283.
47. **Watters, D. J.** 2003. Oxidative stress in ataxia telangiectasia. Redox Rep. **8:**23–29.
48. **Werner, H., E. Karnieli, F. J. Rauscher, and D. LeRoith.** 1996. Wild-type and mutant p53 differentially regulate transcription of the insulin-like growth factor I receptor gene. Proc. Natl. Acad. Sci. U. S. A. **93:**8318–8323.
49. **Xu, Y., T. Ashley, E. E. Brainerd, R. T. Bronson, M. S. Meyn, and D. Baltimore.** 1996. Targeted disruption of ATM leads to growth retardation, chromosomal fragmentation during meiosis, immune defects, and thymic lymphoma. Genes Dev. **10:**2411–2422.
50. **Yamanishi, Y., D. L. Boyle, M. J. Pinkoski, A. Mahboubi, T. Lin, Z. Han, N. J. Zvaifler, D. R. Green, and G. S. Firestein.** 2002. Regulation of joint destruction and inflammation by p53 in collagen-induced arthritis. Am. J. Pathol. **160:**123–130.
51. **Yeung, S. J., J. Pan, and M. H. Lee.** 2008. Roles of p53, MYC and HIF-1 in regulating glycolysis—the seventh hallmark of cancer. Cell. Mol. Life Sci. **65:**3981–3999.
52. **Zheng, S. J., S. E. Lamhamedi-Cherradi, P. Wang, L. Xu, and Y. H. Chen.** 2005. Tumor suppressor p53 inhibits autoimmune inflammation and macrophage function. Diabetes **54:**1423–1428.